A Novel Meteorological Radar Scheme based on the Correlation between Fixed Antennas: a First Look

Marco Antonio Miguel Miranda, José Cândido Silveira Santos Filho, Gustavo Fraidenraich, Michel Daoud Yacoub, João Roberto Moreira Neto, and Yusef Cáceres Zúñiga

***Abstract*— The purpose of this paper is to derive a general analytical expression for the correlation coefficient of signals received by two different antennas as a function of the distance between them (baseline distance), the signal bandwidth, and the antenna beamwidth. The two antennas are supposed to be part of a radar system for detecting meteorological phenomena such as rain and clouds. One of the antennas transmits the radar signal and receives the echoes; the other antenna only receives the echoes. The good functioning of such a radar system depends on the correlation between the two antenna signals. The exact analytical framework derived here has been recently used in practice to assist in the design of a meteorological radar system for Orbisat Indústria e Aerolevantamento S.A.**

***Keywords*— Baseline, correlation coefficient, radar, scattering.**

I. Introduction

A radar (RAdio Detection And Ranging) is a device that detects the presence and range of a target by sending out pulses of high-frequency electromagnetic waves and listening to the echoes from the target. During the last few decades, radar applications have improved considerably and gained widespread use. Traditionally, radars have been used to detect point targets, such as aircrafts, tanks, and ships. But the advance of some techniques has allowed radars to be used for distributed targets as well, such as rain, clouds, and meteorological phenomena in general.

Meteorological radars usually make use of narrow beams. This is achieved with parabolic reflectors of circular aperture illuminated by a horn antenna placed at the focal point of the reflector [1]. To scan the entire sky, the antenna moves in the azimuth and elevation directions in configured steps, a process that may take several minutes depending on the radar setup.

With the early new electronic devices capable of shifting the phase of analog signals, the use of phased-array antennas to detect targets has become feasible. The main advantage of this approach is to reduce at least ten fold the time to scan the entire sky [2]. Electronic scanning is attained by changing the phase and amplitude of each array element, which are regularly spaced by a distance of $\lambda/2$, where λ is the corresponding wavelength of the operating frequency. Another method producing equivalent result is achieved by shifting the nominal operating frequency by a certain amount. Either methods applied to the transmitter and receiver provoke a change in the directivity, as desired.

Another advantage of phased arrays is the capability of performing multitask scanning. Concomitantly with its primary task, namely sky scanning, the phased array can use some of its elements to perform other secondary tasks. For instance, two or three elements inside the array can be selected to estimate the wind velocity, not only radially, but also horizontally and vertically [3], [4]. This method is particularly useful when a high-resolution spatial and temporal estimation is needed, as in the case of a hurricane or tornado.

An alternative technique to detect and measure atmospheric phenomena is based on the use of passive (receiver-only) radars. The setup is composed of a single conventional narrow-beam radar and multiple passive low-gain radars [5]. This technique is low cost, but has difficulties with time and frequency synchronization.

The main purpose of this work is to investigate the feasibility of a new kind of meteorological radar using static antennas. To this end, we analyze the trade-off between baseline distance (B), signal bandwidth (Δf), and antenna beamwidth (θ_{beam}) as they affect the correlation coefficient between the signals received by two static antennas. These signals are echoes caused by a huge number of scatterers involved in a meteorological phenomenon, such as clouds or rain. Therefore, those echoes may be somewhat correlated to each other, and this correlation may provide a basis for a radar detection algorithm. Of course, the higher the correlation, the better the expected performance for the detection algorithm.

II. Radar Concepts and Preliminaries

In this work, we consider a radar device that transmits a linear frequency-modulated signal with a certain bandwidth Δf and receives the echoes from the target. Both operations (transmission and reception) are performed by the same antenna. Therefore, to avoid interference between transmission and reception, these must be performed alternately.

In its way from the transmitted antenna to the target and back to the receiving antenna, the radar signal not only looses power over distance but also has its amplitude and phase affected by the nature of the target. In the case of distributed targets, such as rain and clouds, a huge number of tiny scatterers affect the signal, in a way that a deterministic

João Roberto Moreira Neto, Marco Antonio Miguel Miranda e Yusef Cáceres Zúñiga are with Orbisat Indústria e Aerolevantamento S.A., Campinas, SP, Brazil, Tel: +55 (19) 2101-8844, E-mail: {joao.moreira, marco.miranda,yusef}@orbisat.com.br.

José Cândido Silveira Santos Filho, Gustavo Fraindenraich, and Michel Daoud Yacoub are with the Department of Communications, School of Electrical and Computer Engineering, University of Campinas, 13083-852 Campinas, SP, Brazil, Tel: +55 (19) 3788-5106, Fax: +55 (19) 3289-1395, E-mail:{candido,gf,michel}@decom.fee.unicamp.br.

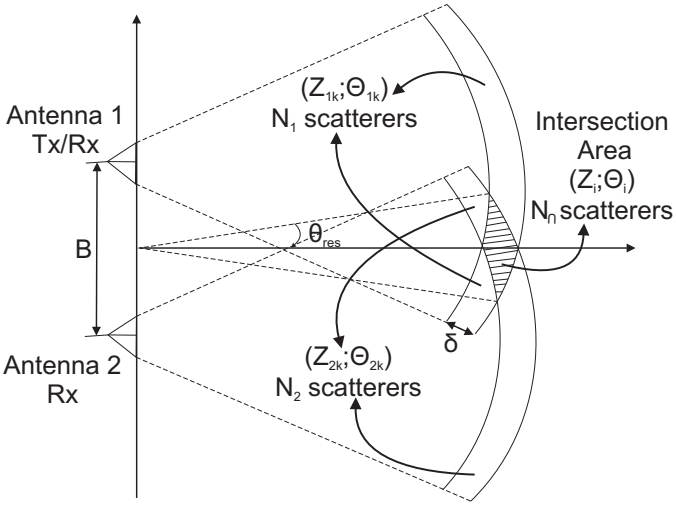

Fig. 1. The radar model.

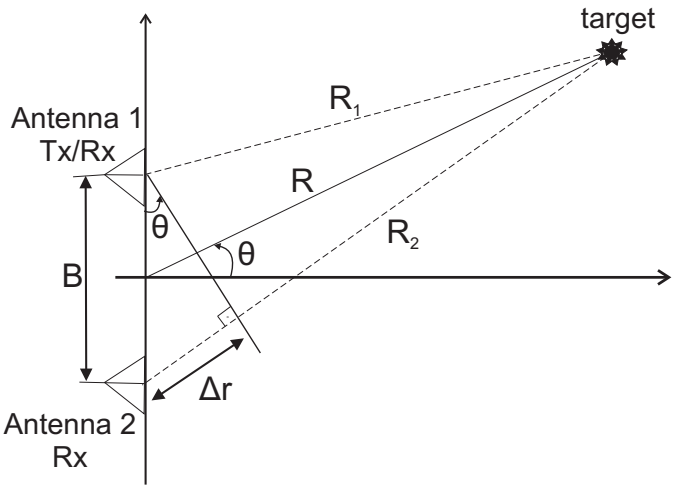

Fig. 2. A target and its coordinates.

analysis is inadequate. Instead, stochastic treatment is used, with the target being described on a probabilistic basis. The stochastic behavior of the radar signal shall be described in the next Section.

After reception, the signal is passed through a matched filter[1], in order to maximize the signal-to-noise ratio. In radar jargon, this operation is known as pulse compression. This way, when the output of the matched filter exceeds a certain threshold, it is very likely that the corresponding received signal was caused by a target echo.

In any radar system, there is a minimum distance between two targets that can de resolved by the radar. This distance is called range resolution (δ). In radar systems with pulse compression, it can be shown that the range resolution is given by [6]

$$\delta = \frac{c}{2\Delta f}, \tag{1}$$

where c is the speed of light. For example, if a radar operates with a bandwidth of 50 MHz, then it can distinguish two targets as close as 3 meters from each other.

Now consider the two-antenna radar system described in Fig. 1. Note that there is a transmitting-and-receiving antenna (antenna 1, Tx/Rx) and a receiving-only antenna (antenna 2, Rx), separated by a baseline distance B. Also note that, for each antenna, the antenna beamwidth and the range resolution define a curved stripped area called range bin. In particular, in the analysis that follows, it is important to know the size of the intersection between the range bins of antenna 1 and antenna 2 (the hachured area in the figure). It is easy to show that the one-sided intersection area (θ_{res}) is given in radians by

$$\theta_{res} = \tan^{-1}\left(\frac{\delta}{B}\right), \tag{2}$$

which, using Eq. (1), gives

$$\theta_{res} = \tan^{-1}\left(\frac{f_0}{2b\Delta f}\right), \tag{3}$$

[1]Here, the matching is performed with respect to the transmitted (not the received) pulse format.

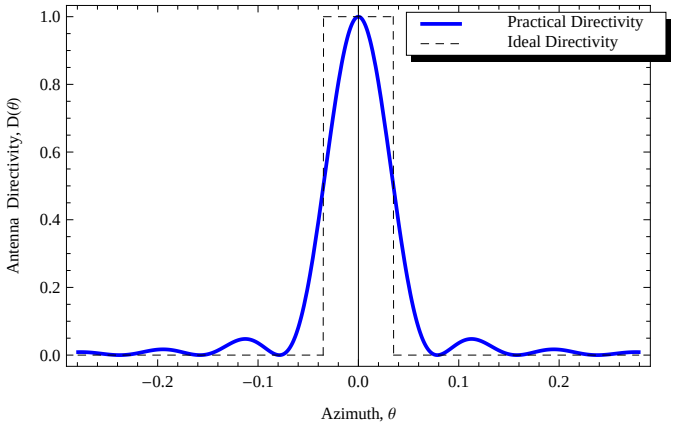

Fig. 3. Directivity patterns for a beamwidth of 4°. (The practical antenna has $N = 25$ elements linearly spaced by $d = \lambda/2$.)

where f_0 is the central frequency of operation and $b \triangleq B/\lambda$ is the normalized baseline for a given wavelength $\lambda = c/f_0$.

Fig. 2 shows a target and its description in cylindrical coordinates. Note that this is a 2-D model, in which the target is identified by two coordinates: azimuth (θ) and range (R). The center of the coordinate system coincides with the center of the antenna axis. Also note that the signal received by antenna 1 travels a total distance of R_1 (from the transmitting antenna 1 to the target) + R_1 (from the target back to antenna 1) $= 2R_1$, whereas the signal received by antenna 2 travels a total distance of R_1 (from the transmitting antenna 1 to the target) $+R_2$ (from the target back to antenna 2) $= R_1+R_2$. Therefore, there is a difference of $\Delta r = R_1 - R_2$ between the distances travelled by the two signals. That difference corresponds to a phase difference of

$$\Delta\phi = \frac{2\pi}{\lambda}\Delta r = \frac{2\pi}{\lambda}B\sin\theta \tag{4}$$

between the signals.

The received signal depends not only on the attenuation over the propagation medium and the amount of reflection from

the target, but also on the directivity pattern of the receiving antenna. In this work, we consider two directivity patterns, as illustrated in Fig. 3. The ideal pattern is described by a door function, which can be written as

$$D(\theta) = \frac{1}{2\theta_{beam}} \left[u\left(\theta + \frac{\theta_{beam}}{2}\right) - u\left(\theta - \frac{\theta_{beam}}{2}\right)\right], \quad (5)$$

where $u(\cdot)$ is the step function. That is, an ideal directive antenna has unity gain within the range $[-\theta_{beam}/2, \theta_{beam}/2]$ and zero gain outside this range. On the other hand, the practical pattern represents a linear array of N antenna elements spaced by a distance d. In this case, the directivity pattern is shown to be given by [7]

$$D(\theta) = \left(\frac{1}{\mathrm{N}} \frac{\sin(\mathrm{N}\pi \frac{d}{\lambda} \sin\theta)}{\sin(\pi \frac{d}{\lambda} \sin\theta)} \right)^2. \quad (6)$$

III. Stochastic Model

The aim of this Section is to develop a stochastic model for the received signals at the two antennas of the radar system described in Fig. 1 and, based on that model, to calculate the correlation coefficient between these two signals.

As mentioned before, the signals received by antenna 1 and antenna 2 are sums of the echoes from a large number of scatterers inside the corresponding range bins. These scatterers represent some possible target (e.g., a cloud) that the radar system is supposed to detect. The contribution from the lth scatterer can be written in complex form as [8]

$$Z_l = A_l e^{j\Phi_l}, \quad (7)$$

where Z_l is a circularly symmetrical, zero-mean, complex Gaussian random variable with variance $2\sigma^2$, the envelope A_l is a Rayleigh random variable with mean power $2\sigma^2$, and the phase $0 < \Phi_l < 2\pi$ is uniformly distributed. Of course, for directive antennas, the azimuth of the scatter impacts the way it is sensed by the antenna. Therefore, in addition to Z_l, we must assign each scatter a second random variable that represents its azimuth, namely Θ_l. The random pair $(Z_l; \Theta_l)$ gives a complete description for the lth scatter. For each scatter, Z_l is assumed to be independent from Θ_l. In addition, the various scatterers are assumed to be independent from each other.

For convenience, we shall distinguish between scatterers inside and outside the intersection area (vide Fig. 1), as follows. Scatterers inside the intersection area shall be denoted by $(Z_i = A_i e^{\Phi_i}; \Theta_i)$, with a single subscript. Scatterers outside the intersection area shall be denoted as $(Z_{1k} = A_{1k} e^{\Phi_{1k}}; \Theta_{1k})$ for antenna 1 and as $(Z_{2k} = A_{2k} e^{\Phi_{2k}}; \Theta_{2k})$ for antenna 2. In addition, we consider that there are $N_\cap$ scatterers inside the intersection area, N_1 scatterers outside the intersection area but still inside the range bin of antenna 1, and N_2 scatterers outside the intersection area but still inside the range bin of antenna 2.

From the above, the received signals at antenna 1 (S_1) and antenna 2 (S_2) can be written as

$$S_1 = \sum_{i=1}^{N_\cap} Z_i \sqrt{D(\Theta_i)} + \sum_{k=1}^{N_1} Z_{1k} \sqrt{D(\Theta_{1k})}, \quad (8)$$

$$S_2 = \sum_{i=1}^{N_\cap} Z_i \sqrt{D(\Theta_i)} e^{j2\pi b \sin\Theta_i} + \sum_{k=1}^{N_2} Z_{2k} \sqrt{D(\Theta_{2k})} \quad (9)$$

Let us summarize the main points:

(i) Z_i, Θ_i, Z_j, Θ_j, Z_{1k}, Θ_{1l}, Z_{1m}, Θ_{1n}, Z_{2o}, Θ_{2p}, Z_{2q}, Θ_{2r} are mutually independent, $\forall i \neq j$, $\forall k \neq m$, $\forall l \neq n$, $\forall o \neq q$, $\forall p \neq r$;

(ii) Z_i, Z_j, Z_{1k}, Z_{1l}, Z_{2m}, Z_{2n} are identically distributed, $\forall i, j, k, l, m, n$;

(iii) Θ_i, Θ_j are identically distributed, $\forall i, j$;

(iv) Θ_{1i}, Θ_{1j} are identically distributed, $\forall i, j$;

(v) Θ_{2i}, Θ_{2j} are identically distributed, $\forall i, j$;

(vi) $\mathrm{E}\{S_1\} = \mathrm{E}\{S_2\} = \mathrm{E}\{Z_i\} = \mathrm{E}\{Z_{1j}\} = \mathrm{E}\{Z_{2k}\} = 0$, $\forall i, j$,

where $\mathrm{E}\{\cdot\}$ denotes expectation.

From (8) and (9), note that both S_1 and S_2 contain information about every scatter $(Z_i; \Theta_i)$ inside the intersection area, $i = 1, \ldots, N_\cap$, and that each scatter is perceived by antenna 2 with a phase shift of $2\pi b \sin\Theta$ with respect to antenna 1. Therefore, in principle, it is possible to improve the radar detection by exploiting the redundant target information into S_1 and S_2. The correlation coefficient

$$\rho \triangleq \frac{\mathrm{COV}\{S_1, S_2\}}{\sqrt{\mathrm{VAR}\{S_1\}\mathrm{VAR}\{S_2\}}} \quad (10)$$

between S_1 and S_2 is a good metric to assess the potentials of such a radar system. ($\mathrm{VAR}\{\cdot\}$ denotes variance and $\mathrm{COV}\{\cdot,\cdot\}$ denotes covariance.) Next, we derive ρ in terms of the physical parameters of the system.

A. Covariance

The covariance of S_1 and S_2 is defined as

$$\mathrm{COV}\{S_1, S_2\} \triangleq \mathrm{E}\{S_1 S_2^*\} - \mathrm{E}\{S_1\}\mathrm{E}\{S_2^*\}. \quad (11)$$

Applying (8) and (9) in (11), and using (i) and (vi), we obtain, after some manipulation, that

$$\mathrm{COV}\{S_1, S_2\} = E\left\{ \sum_{i=1}^{N_\cap} |Z_i|^2 \; D(\Theta_i) e^{-j2\pi b \sin\Theta_i} \right\}. \quad (12)$$

Then, using (i), (ii), and (iii) in (12), we finally obtain

$$\mathrm{COV}\{S_1, S_2\} = N_\cap \mathrm{E}\{|Z_i|^2\} \mathrm{E}\{D(\Theta_i) e^{-j2\pi b \sin\Theta_i}\}. \quad (13)$$

B. Variance

The variance of S_1 is defined as

$$\mathrm{VAR}\{S_1\} \triangleq \mathrm{E}\{S_1 S_1^*\} - \mathrm{E}\{S_1\}\mathrm{E}\{S_1^*\}. \quad (14)$$

Applying equations (8) and (9) in (14), and using (i) and (vi), we obtain, after some manipulation, that

$$\mathrm{VAR}\{S_1\} = \mathrm{E}\left\{ \sum_{i=1}^{N_\cap} |Z_i \sqrt{D(\Theta_i)}|^2 \right\} + \mathrm{E}\left\{ \sum_{k=1}^{N_1} |Z_{1k} \sqrt{D(\Theta_{1k})}|^2 \right\}. \quad (15)$$

Then, using (i), (ii), and (iii) in (15), we obtain

$$\mathrm{VAR}\{S_1\} = \mathrm{E}\{|Z_i|^2\}\left[N_\cap \mathrm{E}\{D(\Theta_i)\} + N_1 \mathrm{E}\{D(\Theta_{1k})\}\right]. \quad (16)$$

Note that Θ_i and Θ_{1j} are non-identically distributed, so that $\mathrm{E}\{D(\Theta_i)\}$ and $\mathrm{E}\{D(\Theta_{1k})\}$ cannot be interchanged. On the other hand, it is possible to use Bayes's Rule to merge those moments into $\mathrm{E}\{D(\Theta)\}$, where Θ is a random variable that represents the azimuth of a scatter inside the range bin of antenna 1, either inside or outside the intersection region. Using this, we finally obtain, after some manipulation, that

$$\mathrm{VAR}\{S_1\} = (N_\cap + N_1)\mathrm{E}\{|Z_i|^2\}\mathrm{E}\{D(\Theta)\}. \quad (17)$$

The same rationale can be also used to obtain the variance of S_2, which gives

$$\mathrm{VAR}\{S_2\} = (N_\cap + N_2)\mathrm{E}\{|Z_i|^2\}\mathrm{E}\{D(\Theta)\}. \quad (18)$$

C. Correlation Coefficient

Now, substituting (13), (17), and (18) in (10), we obtain a general formula for the correlation coefficient ρ, namely

$$\rho = \frac{1}{\sqrt{1+\frac{N_1}{N_\cap}}}\frac{1}{\sqrt{1+\frac{N_2}{N_\cap}}}\frac{\mathrm{E}\{D(\Theta_i)e^{-j2\pi b\sin\Theta_i}\}}{\mathrm{E}\{D(\Theta)\}}. \quad (19)$$

It is possible to write the two expectations in (19) in terms of the probability density function (PDF) of Θ_i, $f_{\Theta_i}(\cdot)$, and the PDF of Θ, $f_\Theta(\cdot)$, yielding

$$\rho = \frac{1}{\sqrt{1+\frac{N_1}{N_\cap}}}\frac{1}{\sqrt{1+\frac{N_2}{N_\cap}}} \times \frac{\int_{-\theta_{res}(b,\Delta f)}^{\theta_{res}(b,\Delta f)} D(\theta_i)e^{-j2\pi b\sin\theta_i} f_{\Theta_i}(\theta_i)d\theta_i}{\int_{-\frac{\pi}{2}}^{\frac{\pi}{2}} D(\theta) f_\Theta(\theta)d\theta}. \quad (20)$$

Note that the integration over θ_i goes from $-\theta_{res}$ to θ_{res} (the angular extension of the intersection area), whereas the integration over θ goes from $-\pi/2$ to $\pi/2$ (the angular extension of the entire range bin). Also note that we have written $\theta_{res}(b,\Delta f)$ instead of just θ_{res}. This is to reinforce here the dependence of θ_{res} on the normalized baseline b and on the signal bandwidth Δf, as shown in (3).

Our new result (20) is a general expression that can be applied to any distribution pattern of the scatterers. In particular, if the scatterers are assumed to be uniformly distributed over the range bin, then Θ becomes uniform from $-\pi/2$ to $\pi/2$, Θ_i becomes uniform from $-\theta_{res}$ to θ_{res}, and $N_1 = N_2$. In addition, the number of scatterers inside a region becomes proportional to size of that region. The intersection region extends from $-\theta_{res}$ to θ_{res}, whereas the non-intersection region extends from $-\pi/2$ to $-\theta_{res}$ and from θ_{res} to $\pi/2$. As a result, N_1 is proportional to θ_{res} in the same way that $N_\cap$ is proportional to $\pi/2 - \theta_{res}$, that is

$$\frac{N_1}{N_\cap} = \frac{\frac{\pi}{2} - \theta_{res}(b,\Delta f)}{\theta_{res}(b,\Delta f)}. \quad (21)$$

Taking all of this into account, (20) specializes into

$$\rho = \frac{2\theta_{res}(b,\Delta f)}{\pi}\frac{\int_{-\theta_{res}(b,\Delta f)}^{\theta_{res}(b,\Delta f)} D(\Theta_i)e^{-j2\pi b\sin\Theta_i}d\Theta_i}{\int_{-\frac{\pi}{2}}^{\frac{\pi}{2}} D(\Theta)d\Theta} \quad (22)$$

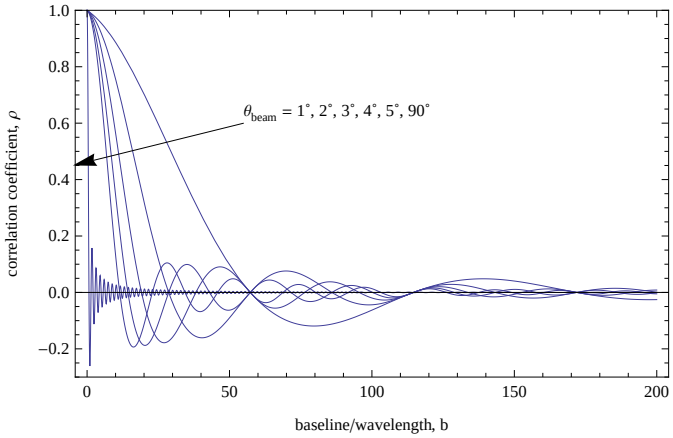

Fig. 4. Correlation coefficient as a function of θ_{beam} ($\Delta f = 50$MHz).

Therefore, in the uniform scenario, the correlation coefficient depends ultimately on the antenna directivity $D(\cdot)$ (and the underlying antenna beamwidth θ_{beam}), the signal bandwidth Δf, and the normalized baseline distance b.

IV. Numerical Results

We now illustrate the use of our new expressions by evaluating the correlation coefficient for a radar system operating at center frequency $f_0 = 9.4$ GHz (X Band). For simplicity, we consider the uniform scenario, for which the correlation coefficient is given by (22). The calculations have been performed numerically using Mathematica.

Fig. 4 shows the effect of the antenna beamwidth θ_{beam}. We consider an ideal antenna, with directivity pattern given by (5), and a signal bandwidth of $\Delta f = 50$ MHz. As a general result, for any value of beamwidth, we observe that the correlation coefficient oscillates around zero and tends to decrease as the baseline distance increases. In addition, we also observe that the correlation coefficient decreases as the beamwidth increases. This is expected, because as the beamwidth increases, the antennas "perceive" more scatterers outside the intersection region, which means more uncommon terms between S_1 and S_2, and, consequently, less correlation.

Fig. 5 shows the effect of the signal bandwidth Δf. We consider an ideal antenna, with directivity pattern given by (5) and an antenna beamwidth of $\theta_{beam} = 1^{\mathrm{o}}$. Again, for any value of signal bandwidth, we observe that the correlation coefficient tends to decrease as the baseline distance increases, becoming less oscillatory as the signal bandwidth increases. In addition, we also observe that the correlation coefficient decreases as the signal bandwidth increases. This is expected, because as the signal bandwidth increases, the size of the intersection region decreases, as predicted by (3), which means less common terms between S_1 and S_2, and, consequently, less correlation.

Finally, Fig. 6 shows the effect of the directivity pattern, contrasting the ideal antenna, with directivity pattern given by (5), against the practical linear antenna array, with directivity pattern given by (6). We consider a signal bandwidth of $\Delta f = 50$ MHz and an antenna beamwidth of $\theta_{beam} = 1^{\mathrm{o}}$. We observe that, in the practical case, the correlation coefficient

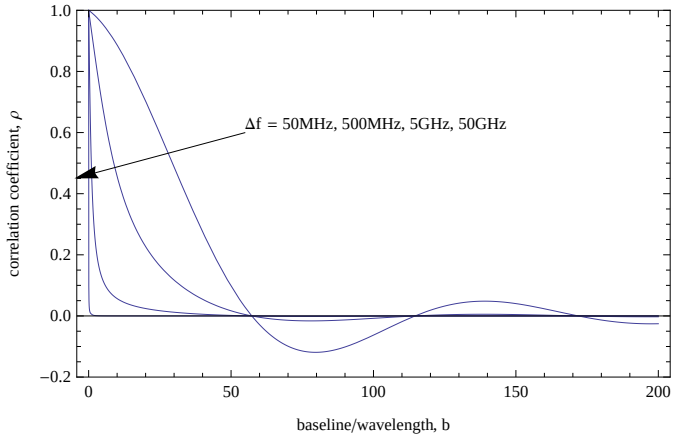

Fig. 5. Correlation coefficient as a function of Δf ($\theta_{beam} = 1^o$).

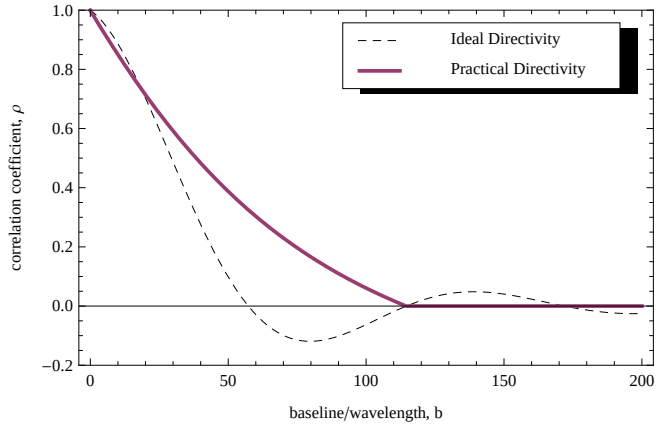

Fig. 6. Correlation coefficient as a function of the directivity pattern: ideal vs. practical (Δf = 50MHz, θ_{beam} = 1^o).

decreases more slowly as the baseline distance increases, but it looses the oscillatory behaviour. As a result, on the one hand, the correlation coefficient for the practical antenna reaches zero at the same baseline distance at which the correlation coefficient for the ideal antenna crosses zero for the second time. On the other, after that distance, the former correlation remains at zero, whereas the latter keeps oscillating.

V. Conclusions

This paper investigated the feasibility of using fixed antennas to implement meteorological radars as an alternative to narrow-beam, moving single-antenna radars. Such an alternative would partition the entire scanning area into appropriate segments, each of which covered by a certain number of fixed antennas. The central idea behind this approach is that fixed widebeam antennas can provide narrowbeam azimuth resolution by exploiting the correlation among their signals due to the intersection of their range bins. The higher the correlation, the better the radar detection capability.

We derived a general expression for the amount of correlation between the signals of two antennas, in terms of the baseline distance (b), the signal bandwidth (Δf), and the antenna directivity ($D(\theta)$). An engineering design specifies a certain minimum θ_{res} to detect the desired target (e.g., $\theta_{res} < 2^o$ for clouds). For a given operation frequency f_0, this minimum θ_{res} implies a minimum value for the product of the normalized baseline distance (b) times the signal bandwidth Δf, as given in (3). On the other hand, as we showed here, the greater the baseline distance or the greater the signal bandwidth, the smaller the correlation coefficient between the antenna signals. This problem can be partially circumvented by using antennas with smaller beamwidths (θ_{beam}). As we showed here, the smaller the beamwidth, the higher the correlation. But again, smaller beamwidth implies the use of more and costlier antennas.

Our new general expressions provide an analytical mathematical framework to help design the radar systems as proposed here. Most importantly, the presented framework has been recently used in practice to assist in the design of a meteorological radar system for Orbisat Indústria e Aerolevantamento S.A.

Acknowledgements

This work was sponsored by Orbisat Industria e Aerolevantamento S.A. and suported by the University of Campinas.

References

[1] Wada, M. and Horikomi, J. and Mizutani, F., *Development of solid-state weather radar*, Radar Conference, 2009 IEEE, pp.1–4, 2009.

[2] Lai, K.H. and Longstaff, I.D. and Callaghan, G.D. *Super-fast scanning technique for phased array weather radar applications*, Radar, Sonar and Navigation, IEE Proceedings, v. 151, n. 5, pp. 271–279, 2004.

[3] Zhang, G. and Doviak, R. J., *Spaced-Antenna Interferometry to Detect and Locate Subvolume Inhomogeneities of Reflectivity: An Analogy with Monopulse Radar.*. J. Atmos. Oceanic Technol., v. 25, n. 11, pp. 1921 – 1938, 2008.

[4] Zhang, G. and Doviak, R.J., *Spaced-antenna interferometry to measure crossbeam wind, shear, and turbulence: Theory and formulation*, J. Atmos. Oceanic Technol., v. 24, n. 5, pp. 791–805, 2010.

[5] Wurman, J. and Heckman, S. and Boccippio, D. *A bistatic multiple-Doppler radar network*, Journal of Applied Meteorology, v. 32, pp. 1802–1802, 1993.

[6] Richards, M.A. and Scheer, J. and Holm, W.A., *Principles of modern radar: Basic principles*, SciTech Pub., 2010.

[7] Balanis, C.A., *Antenna theory: analysis and design*, J. Wiley, New York, 1982.

[8] Cheong, B. L. and Palmer, R. D. and Xue, M., *A time series weather radar simulator based on high-resolution atmospheric models*, Journal of Atmospheric and Oceanic Technology, v. 25, n. 2, pp. 230–243, 2008.